



Bellcomm, Inc.

N70-10460
(ACCESSION NUMBER)

34
(PAGES)

CR-106579
(NASA CR OR TMX OR AD NUMBER)

(THRU)

1
(CODE)

30
(CATEGORY)

FACILITY FORM 602

BELLCOMM, INC.
Washington, D. C. 20024

TR-69-103-7-2

GENERAL CIRCULATION IN THE ATMOSPHERE
OF VENUS DRIVEN BY POLAR AND DIURNAL
VARIATIONS OF SURFACE TEMPERATURE

July 10, 1969

I. O. Bohachevsky
T. T. J. Yeh

Work performed for Manned Space Flight, National Aeronautics and
Space Administration under Contract NASW-417.

ABSTRACT

A three-dimensional model is developed for the representation of circulation in the Venusian atmosphere that includes the effects of both polar cooling and diurnal temperature variation due to the apparent motion of the Sun. The description of the dynamics of the circulation is based on the Boussinesq approximation for a compressible fluid and an analytic expression describing the flow pattern is obtained. The results show that the mean atmospheric motions are essentially meridional, except in a narrow belt near the equator, at a latitude of about 10° , where the direction changes abruptly to zonal. The flow pattern is not symmetrical and rotates about the polar axis of Venus with the period of the Venusian day.

TABLE OF CONTENTS

ABSTRACT

INTRODUCTION

FORMULATION OF THE PROBLEM

THE SOLUTION

DISCUSSION OF RESULTS

CONCLUDING REMARKS

REFERENCES

APPENDIX

FIGURES

DISTRIBUTION LIST

GENERAL CIRCULATION IN THE ATMOSPHERE
OF VENUS DRIVEN BY POLAR AND DIURNAL
VARIATIONS OF SURFACE TEMPERATURE

I. INTRODUCTION

Many space explorations are directed toward planetary studies, especially towards investigations of the two nearest terrestrial planets, Mars and Venus. As part of the effort to improve our understanding of the Venusian environment, this paper examines a three-dimensional model of the general circulation in the atmosphere of Venus.

Many elaborate numerical models have recently been constructed for the description of the general circulation in the atmosphere of Earth^[1,2,3]. However, for other planets the available relevant empirical data are limited and often also uncertain; therefore, use of the above mentioned models, which consume large amounts of computing time, cannot be justified. Even investigation of simpler models of planetary circulation, such as, for example, the model proposed by Leovy and Mintz^[4] or the numerical dishpan experiments performed by Williams^[5] require considerable computing time, rendering parametric studies rather expensive.

We felt, therefore, a need for a simple but meaningful model which would admit an analytic solution and thereby exhibit explicitly the dependence of the flow pattern on different parameters of the problem. Such a solution would facilitate greatly the study of the general characteristics of the atmospheric circulation, provide considerable physical insight into the problem, and assist in planning future, more exact calculations, as well as in evaluating different alternatives for the direct investigation of Venus' meteorology.

Except for a few isolated cases, the possibility of obtaining an explicit solution to a fluid dynamics problem, valid in the large, requires linearity of the governing system of differential equations. Recently Ohring, Tang, and Mariano^[6] have studied the circulation in the atmosphere of Venus with a two-dimensional, time-independent model in which the gas is heated at the bottom by the surface of the planet and the motion is described by a linear version of the Boussinesq approximation

to the equations of fluid dynamics. Their model describes the circulation that is symmetric about the axis joining the subsolar and antisolar points and consists of identical closed cells on vertical planes above each great circle passing through these two points as shown in Figure 1a.

The model of Ref. [6] may also be applied in the case when the flow is symmetric about the polar axis and the temperature on the surface varies with latitude only. The circulation pattern will then consist of cells in the vertical planes above the meridians between the equator and the pole as shown in Figure 1b.

However, because of the slow rotation of Venus, equator to pole and day to night temperature differences can be expected to be comparable in magnitudes and therefore a three-dimensional description is more appropriate. Furthermore, the average wind velocity computed from the above model is of the same order of magnitude as the velocity of the subsolar point along the surface due to the apparent motion of the Sun, and therefore the time independent treatment does not appear to be adequate. In addition, the linearization of the model equations has to be justified.

In view of the above considerations we wish to study the circulation pattern determined by both the polar and the diurnal temperature variations. Consequently, we shall develop a three-dimensional, time-dependent model containing these effects. The temporal variation of temperature will be described by a harmonic behavior with the period of the Venusian day.

We believe that our formulation includes most of the essential features of the dynamics of the atmospheric circulation on Venus. It will be shown that the results obtained with the present model differ considerably from those derived by two-dimensional, time-independent treatments.

The paper is organized as follows: the problem is formulated in Sec. II where the assumptions and approximations are stated. The analysis is described in Sec. III and the results are presented in Sec. IV. Finally, in Sec. V, the validity of the previously made assumptions is discussed, and the consistency of the approximations is demonstrated, using the now available explicit form of the solution.

II. FORMULATION OF THE PROBLEM

A. The Basic Approximations

We shall assume that the vertical extent of the atmosphere in which the circulation is to be determined is much less than the smallest scale height D defined as follows: if f represents any one of the state variables, temperature, pressure, or density, we express it in the form:

$$f(x,y,z,t) = f_m + f_o(z) + f'(x,y,z,t) \quad (1)$$

where f_m denotes the (constant) space and time average of f , f_o is the variation in the absence of any fluid motion, and f' is the variation resulting from convection. Any scale height is then defined by:

$$D = \left| \frac{1}{f_m} \frac{df_o}{dz} \right|^{-1} \quad (2)$$

If d denotes the vertical extent of the region of interest in the atmosphere, the previously stated assumption requires:

$$\frac{d}{D} \ll 1 \quad (3)$$

Clearly, condition (3) depends on the physical parameters as well as on the vertical extent d which must be determined from the solution. After the results are obtained, we shall verify in Sec. V to what extent inequality (3) is satisfied. At the present time, we merely state it as an assumption.

B. The Coordinate System and the Governing Equations

Since the depth of the atmosphere, d , is much smaller than the radius of the planet, R , it is convenient to employ a Cartesian coordinate system with the x -axis pointing east along the equator, the y -axis pointing north along a meridian, and the z -axis pointing upward in the vertical direction. The origin of this coordinate system is placed at the subsolar point at some initial reference time; at this time the antisolar point is at $x = \pi R$, $y = 0$ and the pole is at $y = \pi R/2$.

Assuming inequality (3) to be satisfied, we may apply to the Navier-Stokes equations including a gravitational force the Bossinesq approximation for a compressible fluid, as

derived by Spiegel and Veronis [7]. This approximation is an improvement of the original one introduced by Boussinesq in which the fluid is incompressible and the density change is due to thermal expansion alone giving rise to a buoyancy force. The improvement in Ref. [7] consists of taking into account the additional effect of the compressibility by including, in the energy equation, the work done on the fluid and is therefore a more adequate description of a gas.

With the above stated approximations the system of equations for the flow variables is:

$$\nabla \cdot \underline{v} = 0 \quad (4)$$

$$\frac{D\underline{v}}{Dt} = - \frac{1}{\rho_m} \nabla p - g a \tau + \nu \nabla^2 \underline{v} \quad (5)$$

$$\frac{D\tau}{Dt} + w \left(\frac{\partial T_0}{\partial z} + \frac{g}{c_p} \right) = \kappa \nabla^2 \tau \quad (6)$$

where the vector $\underline{v} = (u, v, w)$ denotes the velocity perturbation about the state of rest, τ is the temperature perturbation, p is the pressure perturbation, ρ_m is a representative mean density, c_p is the specific heat capacity at constant pressure, $\frac{g}{c_p}$ is the adiabatic lapse rate, $g = |\underline{g}|$, \underline{g} is the gravitational acceleration, a is the coefficient of thermal expansion, ν is the eddy coefficient of kinematic viscosity, κ is the eddy coefficient of heat conductivity, and $\frac{D}{Dt}$ denotes the substantial derivative

$$\frac{D}{Dt} = \frac{\partial}{\partial t} + \underline{v} \cdot \nabla \quad (7)$$

Throughout the analysis, the mgs system is used; the units of the various quantities are therefore: ρ (gram/m³), p (gram/m-sec²), τ (°K), \underline{v} (m/sec), g (m/sec²), c_p (m²/sec²-°K), ν and κ (m²/sec), and a (1/°K).

In Eqs. (5) and (6) we have neglected the Coriolis force in comparison to the viscous forces and assumed that the radiative heat transport is small in comparison with the convective transport. The second assumption is a good approximation in the description of the lower atmosphere where convection is the most effective process of energy transfer.

Eddy transport coefficients ν and κ are used because the analysis is intended to apply to large scale mean motions in the atmosphere, where the scale of turbulence is much smaller than the scale of our interest. The implicit assumption here is similar to the Prandtl's mixing length hypothesis, where the apparent coefficients for viscosity and heat conductivity are adopted. Without further justification, empirical constant values for the coefficients ν , κ , a , and c_p will be used.

We are interested in the response of the fluid to the temperature variations on the surface of the planet. We shall consider only those surface temperature changes which are small in comparison to the mean surface temperature T_m ; the experimental evidence indicates that this may be adequate to describe conditions on Venus. We can therefore define a small parameter ϵ as the ratio of the maximum amplitude of the surface temperature variation to T_m , and expand all the dependent variables in powers of ϵ ; for $\epsilon = 0$ the velocity is zero by hypothesis. In this formal expansion procedure, $\underline{v} \cdot \nabla \underline{v}$ and $\underline{v} \cdot \nabla \tau$ terms in Eqs. (5) and (6) are of second order in ϵ and may be neglected in the first approximation. The first order equations are then as follows:*

$$\nabla \cdot \underline{v} = 0 \quad (8)$$

$$\frac{\partial \underline{v}}{\partial t} = - \frac{1}{\rho_m} \nabla p - g \tau + \nu \nabla^2 \underline{v} \quad (9)$$

$$\frac{\partial \tau}{\partial t} + \gamma w = \kappa \nabla^2 \tau \quad (10)$$

where

$$\gamma = \frac{g}{c_p} - \gamma_0 > 0 \quad (11)$$

and γ_0 is the actual lapse rate in the absence of motion.

C. The Boundary Conditions

To complete the formulation of the problem Eqs. (8) (9) and (10) must be supplemented with suitable boundary conditions. At the surface of the planet, $z=0$, the temperature should be determined from the heat flux balance. However, this is a

*All the dependent variables should contain subscripts 1 to indicate first order quantities in ϵ ; however, with no intention to calculate the second order corrections in this report, the subscripts are omitted.

difficult task requiring a solution of the radiative transfer equation; in practice, as an alternative, the surface temperature may be measured. Presently, even such information is very limited as we do not know the entire surface temperature distribution on Venus; at best we can only estimate from available information values at some isolated points, like subsolar and antisolar points and the pole. Our approach therefore, is to assume the temperature distribution as known and to expand it in a Fourier Series. From this series we retain only the fundamental modes along equatorial and polar directions; the former also displays a harmonic time variation. Accordingly, the surface temperature variation is taken to be the following:

$$\tau(x,y,o,t) = T_p \cos \frac{2y}{R} + T_n \cos \left(\frac{x}{R} - \omega_o t \right) \cos \frac{y}{R} \quad (12)$$

where ω_o is the frequency associated with the solar day on Venus; T_p and T_n denote the amplitudes of the polar and diurnal temperature variations. These modes exhibit the required monotone variation between the subsolar and the antisolar points, and between the equator and the pole, as well as the periodic time variation; therefore, they should determine the general features of the circulation pattern. In our linear analysis the effects of higher modes can always be superposed when more detailed information becomes available.

The amplitudes, T_p and T_n , that satisfy the absolute temperature, T_{ss} , at the subsolar point, T_{as} at the antisolar point, and T_{p1} at the pole are:

$$T_n = \frac{1}{2} (T_{ss} - T_{as}) ,$$

$$T_p = \frac{1}{4} (T_{ss} + T_{as}) - \frac{1}{2} T_{p1} ,$$

and the mean temperature T_m is

$$T_m = \frac{1}{4} (T_{ss} + T_{as}) + \frac{1}{2} T_{p1} .$$

The larger of the ratios $\frac{T_p}{T_m}$ or $\frac{T_n}{T_m}$ is the perturbation parameter ϵ introduced in Section IIB.

At $z=0$, the velocity satisfies the usual condition for viscous flows:

$$u = v = w = 0 \quad (13)$$

At large distances away from the surface it is required that all perturbations remain bounded, i.e., as $z \rightarrow \infty$:

$$\begin{aligned} \tau &< \infty \\ u &< \infty \\ v &< \infty \\ w &< \infty \end{aligned} \quad (14)$$

III. THE SOLUTION

Since Eqs. (8) to (10) are linear with constant coefficients it is natural to try the following form of solution:

$$\begin{aligned} \tau &= T e^{\alpha x} e^{\delta y} e^{\beta z} e^{-i\omega t} \\ u &= U \text{ --" --} \\ v &= V \text{ --" --} \\ w &= W \text{ --" --} \\ p &= P \text{ --" --} \end{aligned} \quad (15)$$

where the amplitudes, T , U , V , W , P and the phases α , δ , β , ω are to be determined.

Because the boundary condition (12) is in the form of a sum of polar and night coolings, the solution will consist of two separate contributions due to these two effects; by linearity of the problem, the final results will be superposed.

Substitution of (15) into Eqs. (8) to (10) results in the following linear, homogenous system of algebraic equations for T , U , V , W , and P :

$$\begin{aligned} \alpha U + \delta V + \beta W &= 0 \\ [i\omega + \nu(\alpha^2 + \delta^2 + \beta^2)]U - \frac{\alpha}{\rho_m} P &= 0 \end{aligned}$$

$$\begin{aligned}
 [i\omega + v(\alpha^2 + \delta^2 + \beta^2)]V - \frac{\delta}{\rho_m} P &= 0 \\
 [i\omega + v(\alpha^2 + \delta^2 + \beta^2)]W - \frac{\beta}{\rho_m} P + gaT &= 0 \\
 [i\omega + \kappa(\alpha^2 + \delta^2 + \beta^2)]T - \gamma W &= 0
 \end{aligned} \tag{16}$$

The above equations possess a nontrivial solution if and only if the determinant of the coefficients vanishes; this condition leads to the following relation:

$$(\alpha^2 + \delta^2 + \beta^2) [i\omega + v(\alpha^2 + \delta^2 + \beta^2)][i\omega + \kappa(\alpha^2 + \delta^2 + \beta^2)] + (\alpha^2 + \delta^2) \gamma ga = 0 \tag{17}$$

Since α , δ and ω may be determined from the compatibility requirement for the solution and the boundary conditions, (17) should be considered an equation for β .

With (17) satisfied, the amplitudes are determined from Eqs. (16) as:

$$\begin{aligned}
 U &= - \frac{1}{\gamma} \frac{\alpha\beta}{(\alpha^2 + \delta^2)} [i\omega + \kappa(\alpha^2 + \delta^2 + \beta^2)]T \\
 V &= - \frac{1}{\gamma} \frac{\delta\beta}{(\alpha^2 + \delta^2)} [i\omega + \kappa(\alpha^2 + \delta^2 + \beta^2)]T \\
 W &= \frac{1}{\gamma} [i\omega + \kappa(\alpha^2 + \delta^2 + \beta^2)]T \\
 P &= - \frac{\rho_m}{\gamma} \frac{\beta}{(\alpha^2 + \delta^2)} [i\omega + \kappa(\alpha^2 + \delta^2 + \beta^2)][i\omega + v(\alpha^2 + \delta^2 + \beta^2)]T
 \end{aligned} \tag{18}$$

For the planet Venus the following values of the physical parameters in the above equations are taken as representative [6]:

$$\begin{aligned}
 a &= 2 \times 10^{-3} \text{ per degree} \\
 g &= 8.8 \text{ m/sec}^2 \\
 \gamma &= 2 \times 10^{-3} \text{ }^\circ\text{C/m} \\
 v &= \kappa = 10^3 \text{ m}^2/\text{sec} \\
 R &= 6 \times 10^3 \text{ km} \\
 \omega_0 &= 2\pi/117 \text{ days}
 \end{aligned} \tag{19}$$

It is shown in the Appendix that the solution of Eqs. (8), (9), and (10) subject to the boundary conditions (12), (13), and (14) is:

$$\begin{aligned}
 \tau &= T_n \cos \frac{X}{R} \cos \frac{Y}{R} f_\tau(Z) + T_p \cos \frac{2Y}{R} g_\tau(Z) \\
 u &= \frac{\kappa}{\gamma} R \frac{T_n}{2} b^3 \sin \frac{X}{R} \cos \frac{Y}{R} f_u(Z) \\
 v &= -\frac{\kappa}{\gamma} \frac{R}{2} \left[T_n b^3 \cos \frac{X}{R} \sin \frac{Y}{R} f_v(Z) + T_p c^3 \sin \frac{2Y}{R} g_v(Z) \right] \quad (20) \\
 w &= \frac{\kappa}{\gamma} \left[T_n b^2 \cos \frac{X}{R} \cos \frac{Y}{R} f_w(Z) + T_p c^2 \cos \frac{2Y}{R} g_w(Z) \right] \\
 p &= -2 \frac{\rho_m \nu \kappa}{\gamma} R^2 \left[b^5 T_n \cos \frac{X}{R} \cos \frac{Y}{R} f_p(Z) + \frac{1}{4} c^5 T_p \cos \frac{2Y}{R} g_p(Z) \right]
 \end{aligned}$$

where

$$\begin{aligned}
 f_\tau(z) &= \frac{1}{2} e^{-\frac{b}{2}z} \left[e^{-\frac{b}{2}z} + \cos \frac{\sqrt{3}}{2} bz + \frac{1}{\sqrt{3}} \sin \frac{\sqrt{3}}{2} bz \right] \\
 f_u(z) &= f_v(z) = \frac{-1}{2} e^{-\frac{b}{2}z} \left[e^{-\frac{b}{2}z} - \cos \frac{\sqrt{3}}{2} bz - \frac{1}{\sqrt{3}} \sin \frac{\sqrt{3}}{2} bz \right] \\
 f_w(z) &= \frac{1}{2} e^{-\frac{b}{2}z} \left[e^{-\frac{b}{2}z} - \cos \frac{\sqrt{3}}{2} bz + \frac{1}{\sqrt{3}} \sin \frac{\sqrt{3}}{2} bz \right] \\
 f_p(z) &= \frac{1}{2} e^{-\frac{b}{2}z} \left[e^{-\frac{b}{2}z} + \cos \frac{\sqrt{3}}{2} bz - \frac{1}{\sqrt{3}} \sin \frac{\sqrt{3}}{2} bz \right] \quad (21) \\
 g_\tau(z) &= \frac{1}{2} e^{-\frac{1}{2}cz} \left[e^{-\frac{1}{2}cz} + \cos \frac{\sqrt{3}}{2} cz + \frac{1}{\sqrt{3}} \sin \frac{\sqrt{3}}{2} cz \right] \\
 g_v(z) &= \frac{-1}{2} e^{-\frac{1}{2}cz} \left[e^{-\frac{1}{2}cz} - \cos \frac{\sqrt{3}}{2} cz - \frac{1}{\sqrt{3}} \sin \frac{\sqrt{3}}{2} cz \right] \\
 g_w(z) &= \frac{1}{2} e^{-\frac{1}{2}cz} \left[e^{-\frac{1}{2}cz} - \cos \frac{\sqrt{3}}{2} cz + \frac{1}{\sqrt{3}} \sin \frac{\sqrt{3}}{2} cz \right]
 \end{aligned}$$

$$g_p(z) = \frac{1}{2} e^{-\frac{1}{2}cz} \left[e^{-\frac{1}{2}cz} + \cos \frac{\sqrt{3}}{2} cz - \frac{1}{\sqrt{3}} \sin \frac{\sqrt{3}}{2} cz \right]$$

and

$$b = \left| \begin{array}{c} \left(\frac{2\gamma ga}{R^2 \nu k} \right) \\ \frac{1}{6} \end{array} \right| \quad (22)$$

$$c = \left| \begin{array}{c} \left(\frac{4\gamma ga}{R^2 \nu k} \right) \\ \frac{1}{6} \end{array} \right|$$

In (20) we have introduced a coordinate system moving with the surface velocity of the subsolar point:

$$\begin{aligned} X &= x - u_0 t, \quad u_0 = \omega_0 R \\ Y &= y \\ Z &= z \\ t' &= t \end{aligned} \quad (23)$$

In this coordinate system, the solution appears to be stationary.

For easier visualization the functions $f_\tau, g_\tau, f_p, g_p, f_u, f_v, g_v, f_w$ and g_w are plotted in Figs. 2 and 3.

IV. DISCUSSION OF RESULTS

Even though it is explicit, the solution (20) obtained in the last section is not very revealing by itself. We wish to analyze it in the present section with the intention of obtaining a graphical representation that is easy to visualize and to interpret.

We begin by examining the behavior of the solution in the vertical plane which passes through the subsolar point, antisolar point and the pole. In a coordinate system fixed at the subsolar point, this plane may be represented by the plane $X=0$, with the Y -axis extended beyond the pole to the antisolar point at $Y=\pi R$. It is clear that in the absence of night cooling, the circulation pattern would consist of two cells symmetric about the pole as shown in Fig. 1b. In the general case, however, we should allow the pole to be cooler than both the subsolar and antisolar points, but not by the same amount, and therefore two asymmetric circulation cells are to be expected. The boundary between these two cells may be determined approximately from the vanishing of the y component of the velocity, because they are separated by a dividing streamline along which the flow is predominantly in the vertical direction.

In the plane $X = 0$, since $c^3 = \sqrt{2}b^3$, we have

$$v = - \frac{\kappa}{\gamma} \frac{R}{2} T_n b^3 \sin \frac{Y}{R} f_v(Z) \left[1 + 2\sqrt{2} \theta \cos \frac{Y}{R} \frac{g_v(Z)}{f_v(Z)} \right] \quad (24)$$

where $\theta \equiv \frac{T_p}{T_n}$ is a measure of the relative importance of polar and night coolings. From Fig. 3 we observe that

$$\frac{g_v(Z)}{f_v(Z)} \approx 1$$

and therefore the condition $v = 0$ leads to

$$1 + 2\sqrt{2} \theta \cos \frac{Y}{R} = 0. \quad (25)$$

For a typical value of θ , say 1.5, we find

$$\frac{Y}{R} \approx 105^\circ$$

i.e., the point in question is located on the night side 15° off the pole. We shall refer to it as the "circulation pole" (CP) in analogy to the magnetic pole. Thus, the circulation is not symmetrical about the pole because the thermal driving force is larger on the day side than on the night side.

The occurrence of two asymmetrical circulation cells in the plane of symmetry of the flow pattern is the first consequence of the three-dimensionality of the analysis. The structure of the flowfield over the remainder of the globe will be examined in the next paragraph. Here we only observe that, as the polar cooling T_p tends to zero, our solution reduces to the two-dimensional symmetric circulation between the subsolar and anti-solar points investigated previously in Ref. [6]; as the night cooling T_n tends to zero the circulation reduces to the corresponding pattern symmetric about the polar axis. A graph of the position of the circulation pole as function of θ is shown in Figure 4.

We will now turn our attention to the examination of flow behavior in horizontal planes $z = \text{const}$. From Fig. 3 we see that the horizontal velocity components u and v reverse directions at an altitude of about 20 km. The direction fields $\text{arc tg } \frac{v}{u}$, constructed at two altitudes, $z = 10$ km and $z = 30$ km, are shown on the Mercator projection of the globe in Fig. 5. The

result demonstrates that the directions are, to within only a few degrees, almost exactly reversed for all x and y . This indicates that the trajectories of fluid parcels very nearly lie on surfaces, not necessarily planes, that extend vertically upward from the surface of the planet. These surfaces, together with the information about the circulation pole, are shown schematically in Fig. 6 that may conveniently be thought of as the inverse of the Mercator projection. We see that, depending on the altitude level, the gas motion is mainly along the meridians, away from or towards the pole, to within 5° or 10° latitude where it turns abruptly into the equatorial direction. We wish to note here that the curves in Fig. 6 are not the trajectories of individual fluid parcels but, in the Euler's formulation, the projections of the local velocity onto the surface of the planet.

The most effective way of discussing any direction field is to examine its singularities. In our case the two-dimensional direction field in a plane $z = \text{const}$ is given by

$$\phi = \text{arc tg } \frac{v}{u} \quad (26)$$

where

$$\frac{v}{u} = \frac{\text{tg } \frac{Y}{R}}{\text{tg } \frac{X}{R}} + 2\sqrt{2} \theta \frac{g_u}{f_u} \cdot \frac{\sin \frac{Y}{R}}{\sin \frac{X}{R}} \quad (27)$$

The singularities of this field, i.e., points where v and u vanish simultaneously, are at the subsolar and anti-solar points and at the circulation pole. From the examination of the limiting behavior of the quotient $\frac{v}{u}$ at these points we determine that at altitudes between 0 and about 20 km (see Fig. 3), the subsolar point and the circulation pole are a sink and a source respectively; the roles become reversed above 20 km. The antisolar point is a saddle point for all altitudes. The behavior of the field at the singular points and in between is shown schematically in Fig. 7. An immediate consequence of this behavior is the fact that, unlike in the two-dimensional case, the circulation cells are not closed at the antisolar point. Rather, they bend there abruptly into the equatorial direction and extend all the way to the subsolar point.

Combining the information contained in Figs. 4 through 7 we obtain Fig. 8 which is a three-dimensional sketch of the circulation pattern. The shaded strips represent schematically

individual circulation cells. It is seen that the gas rises at the subsolar point and then flows away from it horizontally in all directions. Those elements which are nearly in a meridian plane will approach the circulation pole without much change in direction; those which are nearly in the equatorial plane will continue in it for some distance and then make sharp turns into meridional directions. The closer the cell approaches the anti-solar point the sharper the turn. Above the altitude of about 20 km the flow directions are reversed to complete the pattern. This flow pattern may be best visualized by folding Fig. 8 along the diameter connecting the subsolar and antisolar points so that the equatorial and meridional planes are perpendicular. We emphasize here again that the lines in Fig. 8 are not the trajectories of fluid parcels but rather indicate the results of simultaneous measurements of the horizontal flow directions at any given time.

For an observer fixed on the surface of the planet, the flow pattern depicted in Fig. 8 rotates about the pole with the Sun at the frequency ω_0 .

For the values of parameters listed in (19), and $T_n = 15^\circ\text{K}$, $T_p = 22.5^\circ\text{K}$, $T_m = 600^\circ\text{K}$, our solution yields the following typical magnitudes for the velocity components:

$$u = 15 \text{ km/hr.}$$

$$v = 35 \text{ km/hr.}$$

$$w = .15 \text{ km/hr.}$$

These magnitudes agree quite well with previous computations [6,8] from two-dimensional treatments, even though the flow patterns are completely different.

V. CONCLUDING REMARKS

Having an explicit expression for the solution and a visualization of its global behavior we are now in a position to examine critically the various approximations involved.

The Boussinesq approximation is probably the weakest assumption in the analysis. It is strictly valid only for motions with vertical extents which are smaller than any appropriately defined scale height of the fluid. When the scale height is defined by Eq. (2) on the basis of temperature we obtain, for the lapse rate of $8^\circ/\text{km}$ and a mean temperature

of 600°K , $D = 75$ km. Since, from Figure 3, d is about 50 km the assumption expressed by inequality (3) is only marginally satisfied. However, the lapse rate of $8^\circ/\text{km}$ and the atmosphere depth of 50 km are both conservative values and therefore the actual situation may be more favorable. The scale height based on pressure or density from a hydrostatic calculation is only about 15 km and our solution is, strictly speaking, not valid beyond this range. Nevertheless, as argued by Goody and Robinson^[9], the Boussinesq approximation may still be valid if appropriate local mean values for pressure and density are employed. In spite of the above uncertainty, our approach yields a solution which reflects many qualitative features of the problem.

Now, we wish to examine the question of the nonlinear transport terms in more detail. Within the framework of our expansion procedure, the ratio of the neglected momentum convective terms to the retained viscous terms is proportional

to $\epsilon \frac{\underline{v} \cdot \nabla \underline{v}}{\nu \nabla^2 \underline{v}}$. From the explicit expressions for the solution

(20), we see that $\frac{\underline{v} \cdot \nabla \underline{v}}{\nu \nabla^2 \underline{v}}$ is bounded for all x , y , and z .

Heat transport terms are estimated similarly. For the particular values of the parameters that characterize the atmosphere of Venus, (19), and $T_n = 15^\circ\text{K}$, $T_p = 22.5^\circ\text{K}$, $T_m = 600^\circ\text{K}$, the numerical values of $\epsilon (\underline{v} \cdot \nabla \underline{v})$, amount to about 10% of the viscous terms, and $\epsilon (\underline{v} \cdot \nabla \tau)$ to about 15% of the heat conduction term. Thus the results are consistent with the approximations of the analysis.

We may also gain better understanding of the circulation phenomena described in this analysis from the following two considerations. First, the gradient operator and the velocity vector of a fluid circulating along closed, convex streamlines in a plane are nearly perpendicular and therefore their scalar product is small (it would vanish identically in the case of circular symmetry). As mentioned in Sec. IV, and as seen from the results presented in Figs. 6 and 8 the flow described by our solution takes place predominantly in vertical planes and therefore the above argument applies approximately. This reasoning has been described in more detail by Bohachevsky^[8].

Second, the present problem differs essentially from the classical Benard problem in which thermal convection results from the instability caused by an excessive vertical temperature

lapse and the nonlinear terms are required to check the growth of the instabilities. In our problem the motion is generated and sustained by the horizontal temperature gradient along the bottom surface perpendicular to the force of gravity. This is contained in the assumption that the unperturbed solution is the state of rest. The linear description therefore appears adequate provided the surface temperature variations are small compared to the mean temperature.

In the present paper we have assumed that the atmosphere is heated by a prescribed temperature distribution over the surface of the planet, and we have described the resulting circulation pattern in a Cartesian coordinate system. We have also developed a model simulating some optical properties of the atmosphere, in which the thermal driving force is applied not only at the bottom but also at an arbitrary altitude level in the interior of the atmosphere. This model, which has been used in connection with a two-dimensional circulation pattern, is described in a separate Bellcomm document [8].

I. O. Bohachevsky

I. O. Bohachevsky

T. T. J. Yeh

T. T. J. Yeh

1014-IOB
TTJY-1mc

Attachment
Appendix
Figures 1 through 8

BELLCOMM, INC.

REFERENCES

1. Smagorinsky, J., Manabe, S., Holloway, L. J., Jr., "Numerical Results from a Nine-Level General Circulation Model of the Atmosphere," Monthly Weath. Rev., 93, 727-768, 1965.
2. Sadourny, R., Arakawa, A. and Mintz, Y., "Integration of the Nondivergent Barotropic Vorticity Equation with an Icosahedral-Hexagonal Grid for a Sphere," Monthly Weath. Rev., 96, 351-356, 1968.
3. Kirihara, Y. and Holloway, L. J., Jr., "Numerical Integration of a Nine-Level Global Primitive Equations Model Formulated by the Box Method," Monthly Weath. Rev., 95, 509-530, 1967.
4. Leovy, C. B. and Mintz, Y., "A Numerical General Circulation Experiment for the Atmosphere of Mars," Rand Corp. Memo. RM-5110-NASA, Dec. 1966.
5. Williams, G. P., "Thermal Convection in a Rotating Fluid Annulus": Part I and II, J. Atm. Sci., 24, 144-161 and 162-174, 1967.
6. Ohring, G., Tang, W., and Mariano, J., "Planetary Meteorology," NASA CR-280, 1965.
7. Spiegel, E. A., and Veronis, G., "On Boussinesq Approximation for a Compressible Fluid," Astrophys. J., 131, 442-447, 1960.
8. Bohachevsky, I. O., "A Linear Model of Atmospheric Circulation," Bellcomm TM-69-1014-4, January 31, 1969.
9. Goody, R. M., and Robinson, A. R., "A Discussion of the Deep Circulation of the Atmosphere of Venus," Astrophys. J., 146, 339-355, 1966.

APPENDIX

In the following subsections we present the details of the computations of polar and night cooling contributions.

A. Polar Cooling

For the fundamental mode compatible with the first term in the boundary condition (12), which represents the polar cooling, we have the following values for α , δ , and ω :

$$\begin{aligned}\alpha &= 0 \\ \delta &= \pm \frac{21}{R} \\ \omega &= 0\end{aligned}\tag{A1}$$

The expression for β from Eq. (17) is now

$$\beta^2 = \left[- \frac{(\alpha^2 + \delta^2) \gamma g a}{\nu \kappa} \right]^{\frac{1}{3}} (1)^{\frac{1}{3}} - (\alpha^2 + \delta^2)\tag{A2}$$

With the values of the parameters specified by (19) and (A1) the ratio of the second to the first term on the right hand side of (A2) is about 10^{-5} . Therefore $(\alpha^2 + \delta^2)$ on the right hand side of (A2) may be neglected to yield:

$$\beta = c(1)^{1/6}\tag{A3}$$

where:

$$c = \left| \left(\frac{4 \gamma g a}{R^2 \nu \kappa} \right)^{\frac{1}{6}} \right|\tag{A4}$$

The six values of β are therefore given by:

$$\beta_k = c e^{i\pi k/3}, \quad k = 1, 2, \dots, 6\tag{A5}$$

With the same approximation as in (A3), $\delta \ll \beta$, the solution is now given by:

$$\tau = \sum_{j=1}^2 \sum_{k=1}^6 T_k e^{\delta_j y} e^{\beta_k z}$$

$$u = 0$$

$$v = -\frac{\kappa}{\gamma} \sum_{j,k} \frac{1}{\delta_j} \beta_k^3 T_k e^{\delta_j y} e^{\beta_k z} \quad (\text{A6})$$

$$w = \frac{\kappa}{\gamma} \sum_{j,k} \beta_k^2 T_k e^{\delta_j y} e^{\beta_k z}$$

$$p = \frac{\rho_m \nu \kappa}{\gamma} \sum_{j,k} \frac{1}{\delta_j^2} \beta_k^5 T_k e^{\delta_j y} e^{\beta_k z}$$

The boundary condition at $z \rightarrow \infty$ requires that $T_k = 0$ when $\text{Re } \beta_k > 0$. Therefore $T_1 = T_5 = T_6 = 0$. The boundary conditions at the surface $z = 0$ and Eq. (A6) then lead to the following algebraic equations for the remaining T_k 's:

$$T_3 + T_4 + T_2 = T_p$$

$$\beta_3^2 T_3 + \beta_4^2 T_4 + \beta_2^2 T_2 = 0 \quad (\text{A7})$$

$$\beta_3^3 T_3 + \beta_4^3 T_4 + \beta_2^3 T_2 = 0$$

The solution of (A7) is:

$$T_3 = \frac{1}{2} T_p$$

$$T_4 = \frac{1}{4} \left(1 + \frac{1}{\sqrt{3}} i \right) T_p \quad (\text{A8})$$

$$T_2 = \frac{1}{4} \left(1 - \frac{1}{\sqrt{3}} i \right) T_p$$

The primary flow variables are now given by:

$$\tau = T_p \cos \frac{2y}{R} g_\tau(z)$$

$$u = 0$$

$$v = -\frac{\kappa R}{\gamma} \frac{T_p}{2} c^3 \sin \frac{2y}{R} g_v(z) \quad (A9)$$

$$w = \frac{\kappa}{\gamma} T_p c^2 \cos \frac{2y}{R} g_w(z)$$

$$p = -\frac{1}{2} \frac{\rho \pi^{1/2} \kappa}{\gamma} R^2 c^5 T_p \cos \frac{2y}{R} g_p(z)$$

where

$$\begin{aligned} g_\tau(z) &= \frac{1}{2} e^{-\frac{1}{2}cz} \left[e^{-\frac{1}{2}cz} + \cos \frac{\sqrt{3}}{2} cz + \frac{1}{\sqrt{3}} \sin \frac{\sqrt{3}}{2} cz \right] \\ g_v(z) &= -\frac{1}{2} e^{-\frac{1}{2}cz} \left[e^{-\frac{1}{2}cz} - \cos \frac{\sqrt{3}}{2} cz - \frac{1}{\sqrt{3}} \sin \frac{\sqrt{3}}{2} cz \right] \quad (A10) \\ g_w(z) &= \frac{1}{2} e^{-\frac{1}{2}cz} \left[e^{-\frac{1}{2}cz} - \cos \frac{\sqrt{3}}{2} cz + \frac{1}{\sqrt{3}} \sin \frac{\sqrt{3}}{2} cz \right] \\ g_p(z) &= \frac{1}{2} e^{-\frac{1}{2}cz} \left[e^{-\frac{1}{2}cz} + \cos \frac{\sqrt{3}}{2} cz - \frac{1}{\sqrt{3}} \sin \frac{\sqrt{3}}{2} cz \right] \end{aligned}$$

The plots of the functions g_τ , g_p , g_v , and g_w are shown in Figs. 2 and 3.

B. Night Cooling

For the fundamental mode compatible with the second term in the boundary condition (12), which represents the effect of the night cooling, we obtain the following values of α , δ , and ω :

$$\begin{aligned}\alpha_{1,3} &= \alpha_{2,4} = \pm \frac{1}{R} \\ \delta_{1,3} &= \delta_{2,4} = \pm \frac{1}{R} \\ \omega &= \omega_0\end{aligned}\tag{A11}$$

The value of β may now be determined from (17) which is a cubic equation for β^2 . In order to simplify the algebra let us compare the terms ω and $\kappa\beta^2$. If we take $\omega = \omega_0 = \frac{2\pi}{117 \text{ days}}$, κ from Eq. (19), and β calculated in the previous section for $\omega=0$, we find that

$$\frac{\omega}{\kappa\beta^2} \approx 6 \times 10^{-2}$$

Therefore, as a first approximation, in our linear model, ω may be neglected in calculating β . Physically, this means that the change in the perturbed atmosphere by conduction follows the change at the surface without appreciable time delay, since $(\kappa\beta^2)^{-1}$ is the characteristic conduction time. The resulting β is

$$\beta = b(1)^{1/6}\tag{A12}$$

$$b = \left| \left(\frac{2\gamma g a}{R^2 \nu \kappa} \right)^{1/6} \right|\tag{A13}$$

The six possible values of β therefore are:

$$\beta_k = b e^{i\pi k/3}, \quad k = 1, 2, \dots, 6\tag{A14}$$

Thus, following the same procedure as in the polar cooling, we find that in the present case of night cooling the solution is given by:

$$\begin{aligned}\tau &= T_n \cos\left(\frac{x}{R} - \omega_0 t\right) \cos\frac{y}{R} f_\tau(z) \\ u &= -\frac{\kappa}{\gamma} R \frac{T_n}{2} b^3 \sin\left(\frac{x}{R} - \omega_0 t\right) \cos\frac{y}{R} f_u(z)\end{aligned}$$

$$v = -\frac{\kappa}{\gamma} R \frac{T_n}{2} b^3 \cos\left(\frac{X}{R} - \omega_0 t\right) \cos\frac{Y}{R} f_v(z) \quad (A15)$$

$$w = \frac{\kappa}{\gamma} T_n b^2 \cos\left(\frac{X}{R} - \omega_0 t\right) \cos\frac{Y}{R} f_w(z)$$

$$p = -2\frac{\rho_m v \kappa}{\gamma} R^2 b^5 T_n \cos\left(\frac{X}{R} - \omega_0 t\right) \cos\frac{Y}{R} f_p(z)$$

where

$$f_\tau(z) = \frac{1}{2} e^{-\frac{b}{2}z} \left[e^{-\frac{b}{2}z} + \cos\frac{\sqrt{3}}{2}bz + \frac{1}{\sqrt{3}} \sin\frac{\sqrt{3}}{2}bz \right]$$

$$f_u(z) = f_v(z) = -\frac{1}{2} e^{-\frac{b}{2}z} \left[e^{-\frac{b}{2}z} - \cos\frac{\sqrt{3}}{2}bz - \frac{1}{\sqrt{3}} \sin\frac{\sqrt{3}}{2}bz \right]$$

$$f_w(z) = \frac{1}{2} e^{-\frac{b}{2}z} \left[e^{-\frac{b}{2}z} - \cos\frac{\sqrt{3}}{2}bz + \frac{1}{\sqrt{3}} \sin\frac{\sqrt{3}}{2}bz \right]$$

$$f_p(z) = \frac{1}{2} e^{-\frac{b}{2}z} \left[e^{-\frac{b}{2}z} + \cos\frac{\sqrt{3}}{2}bz + \frac{1}{\sqrt{3}} \sin\frac{\sqrt{3}}{2}bz \right]$$

The above expressions may be simplified somewhat by the introduction of a coordinate system (23) which is moving with the surface velocity of the subsolar point. In this representation the pattern appears to be stationary:

$$\tau = T_n \cos\frac{X}{R} \cos\frac{Y}{R} f_\tau(z)$$

$$u = -\frac{\kappa}{\gamma} R \frac{T_n}{2} b^3 \cos\frac{X}{R} \sin\frac{Y}{R} f_u(z)$$

$$v = -\frac{\kappa}{\gamma} R \frac{T_n}{2} b^3 \cos\frac{X}{R} \sin\frac{Y}{R} f_v(z) \quad (A16)$$

$$w = \frac{\kappa}{\gamma} T_n b^2 \cos\frac{X}{R} \cos\frac{Y}{R} f_w(z)$$

$$p = -2\frac{\rho_m v \kappa}{\gamma} R^2 b^5 T_n \cos\frac{X}{R} \cos\frac{Y}{R} f_p(z)$$

For easier visualization the functions f_{τ} , f_p , f_v , and f_w are plotted in Figs. 2 and 3.

Making use of the superposition principle the final solution, consisting of the sum of the contributions due to polar and night coolings, is given by (20) in Sec. III.

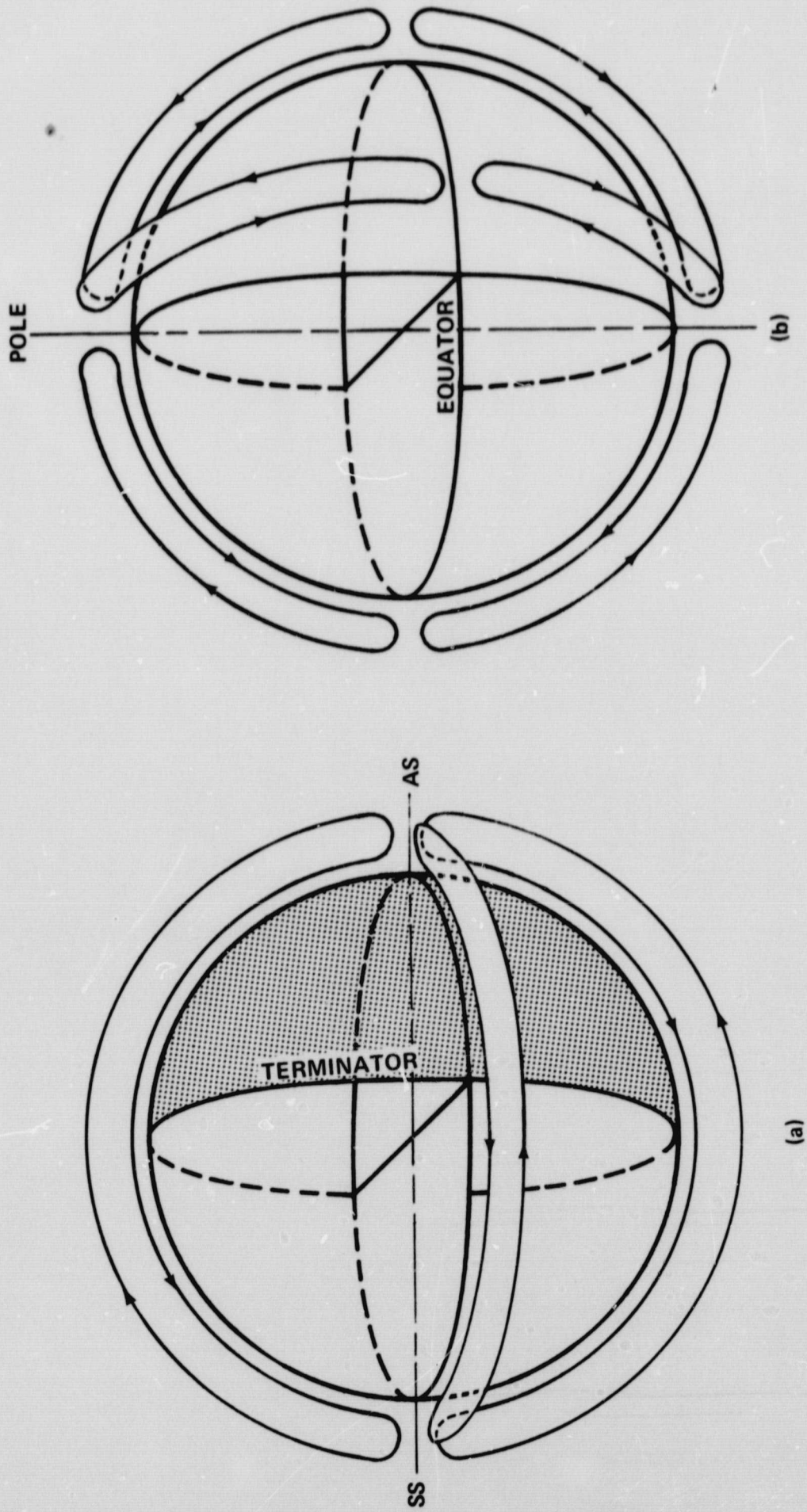


FIGURE 1 - CIRCULATION PATTERNS BASED ON TWO-DIMENSIONAL MODEL.
 (a) TEMPERATURE DIFFERENCE IS BETWEEN SUBSOLAR AND
 ANTISOLAR POINTS, (b) TEMPERATURE DIFFERENCE IS BETWEEN
 EQUATOR AND POLE.

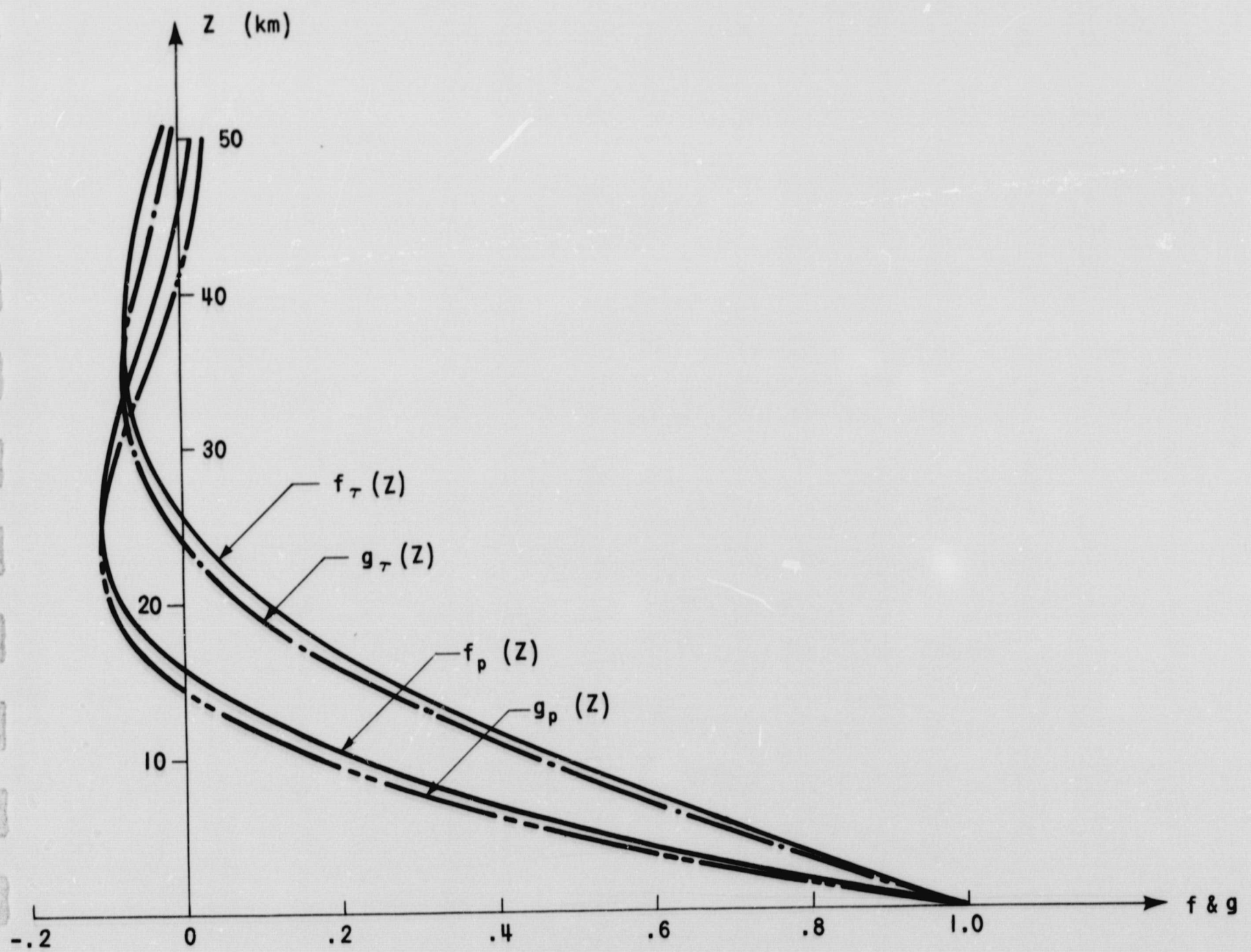


FIGURE 2 - THE Z - DEPENDENCES OF TEMPERATURE AND PRESSURE VARIATIONS

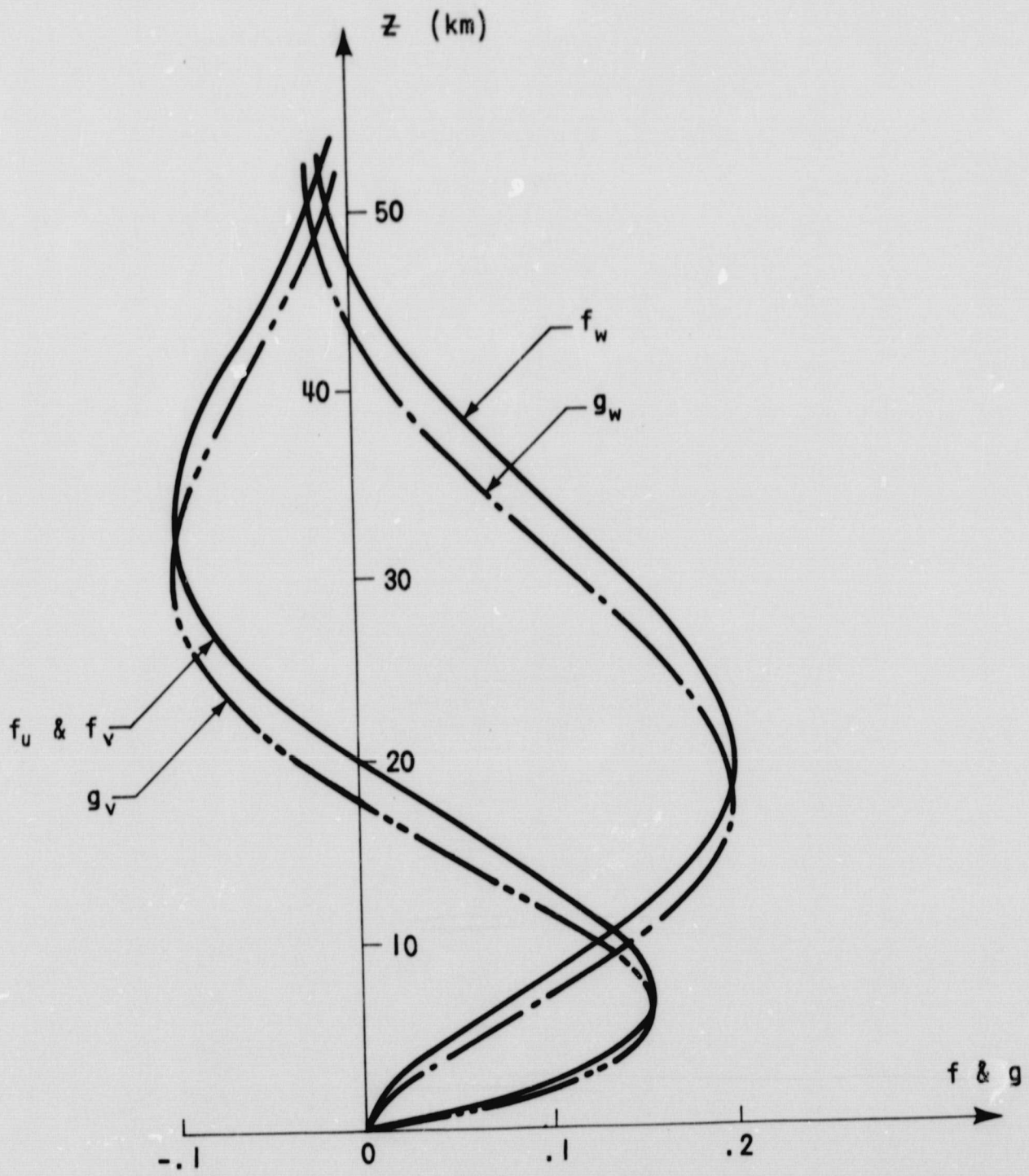


FIGURE 3 - THE Z-DEPENDENCES OF VELOCITY VARIATIONS

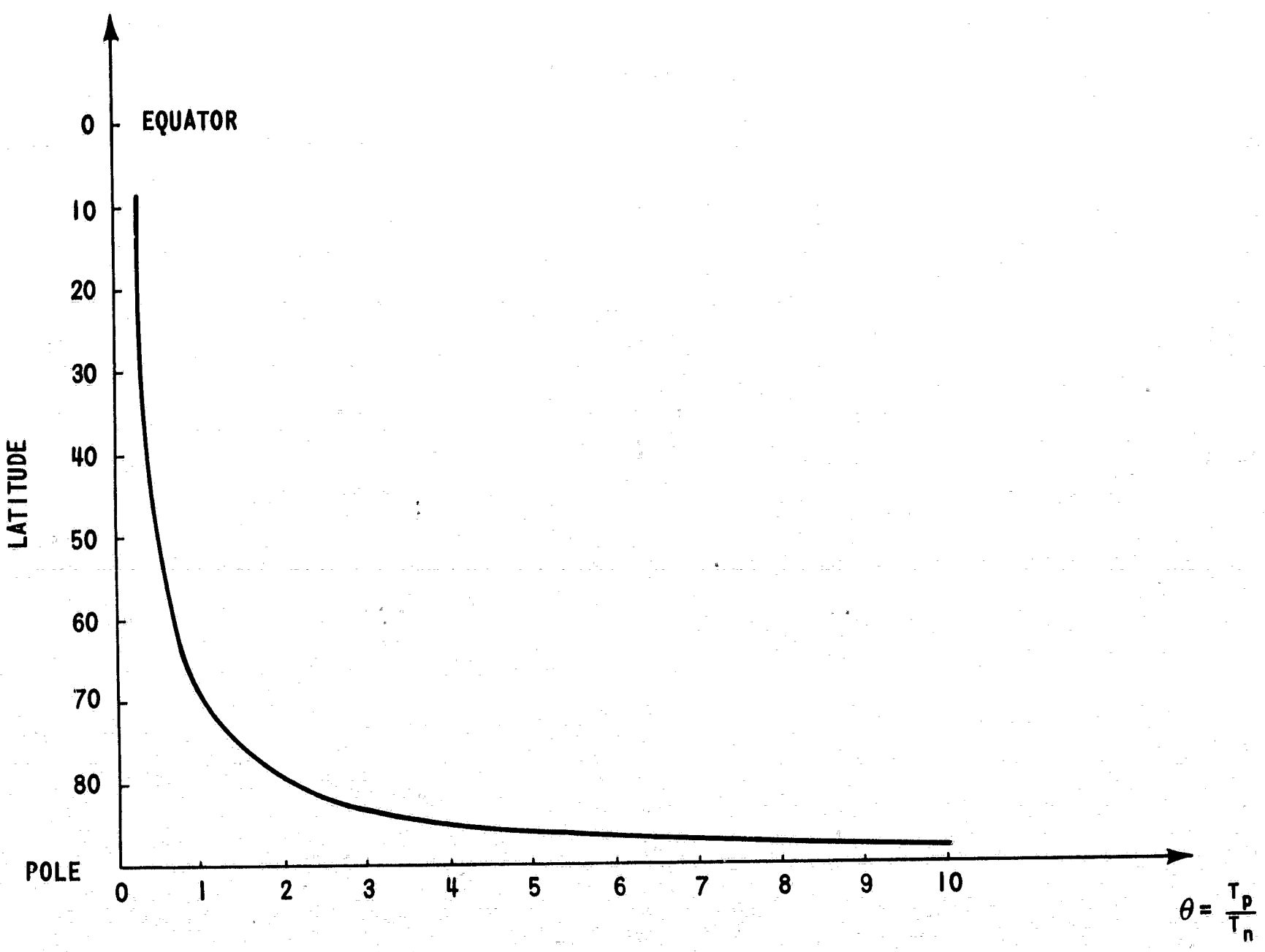


FIGURE 4 - LOCATION OF CIRCULATION POLE AS A FUNCTION OF θ

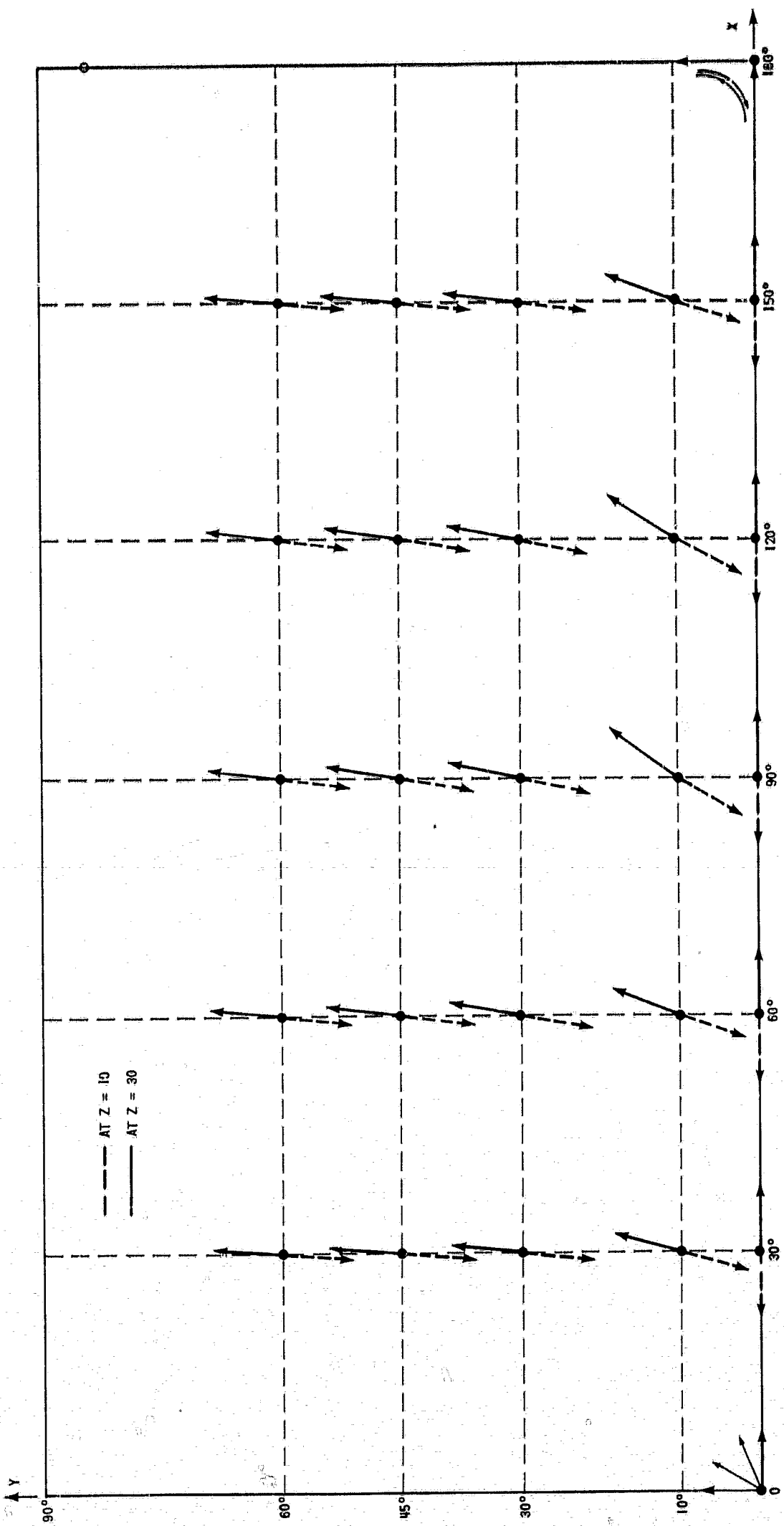
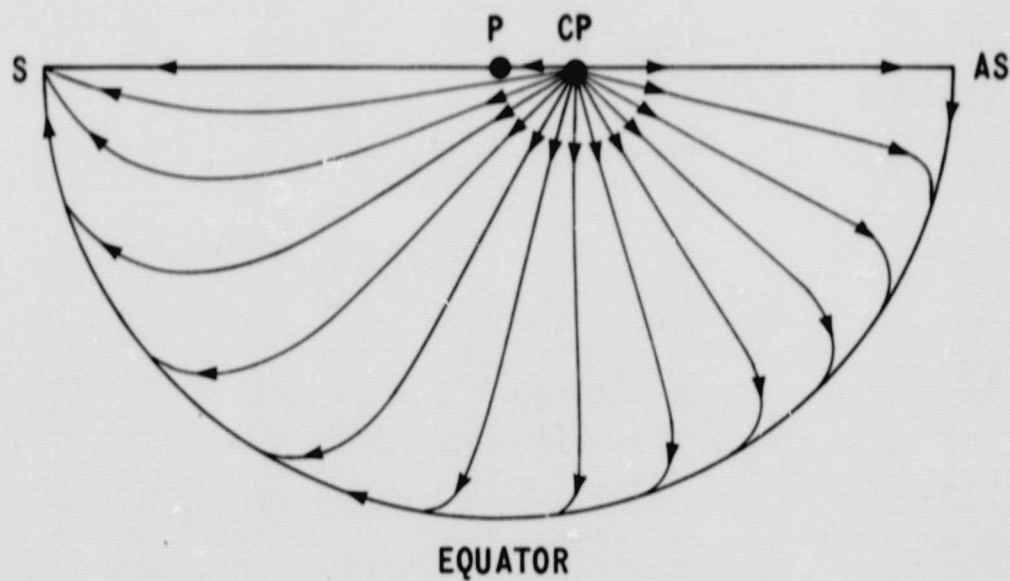
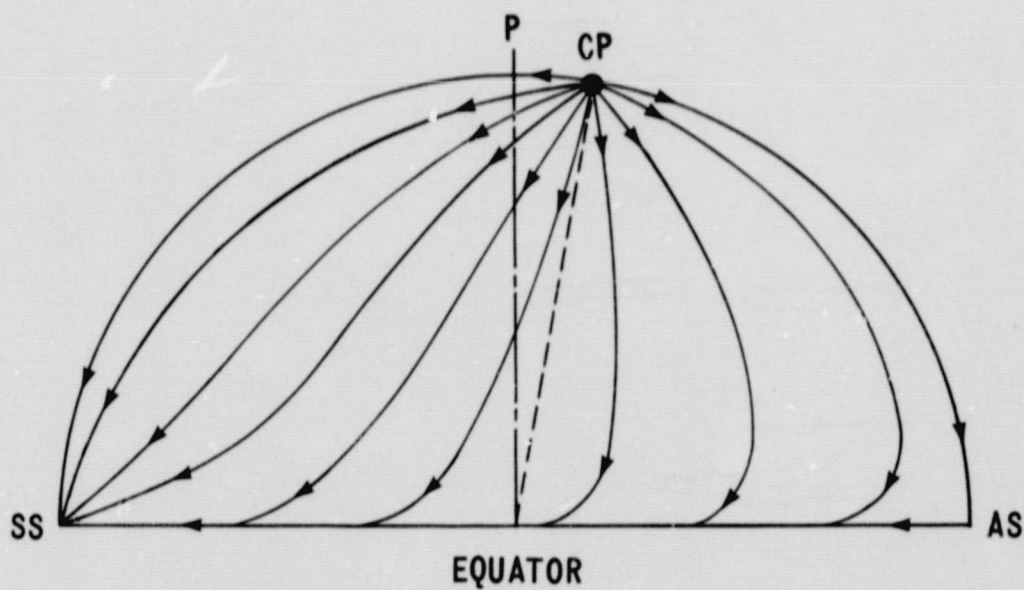


FIGURE 5 - DIRECTION FIELD OF THE HORIZONTAL VELOCITY COMPONENTS

SS - SUBSOLAR POINT
AS - ANTISOLAR POINT
CP - CIRCULATION PCLE
P - POLE



TOP VIEW



FRONT VIEW

FIGURE 6- TOP AND FRONT VIEWS OF FLOW DIRECTIONS
IN THE NORTHERN HEMISPHERE AT $Z = 10$ KM.
AT $Z = 30$ KM THE FLOW DIRECTIONS ARE REVERSED

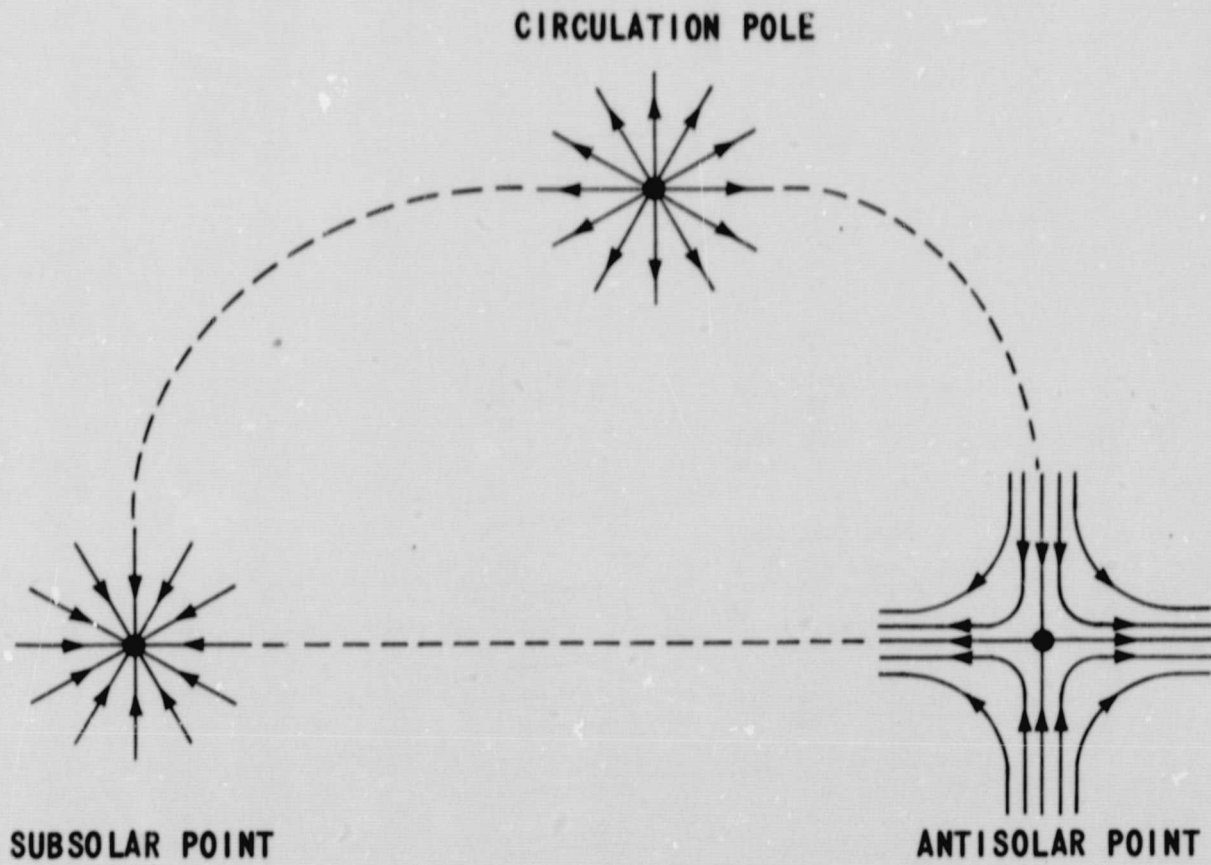


FIGURE 7 - FLOW BEHAVIORS NEAR SUBSOLAR POINT, ANTISOLAR POINT, AND CIRCULATION POLE AT $Z = 10$ KM. FLOW DIRECTIONS ARE REVERSED AT $Z = 30$ KM.

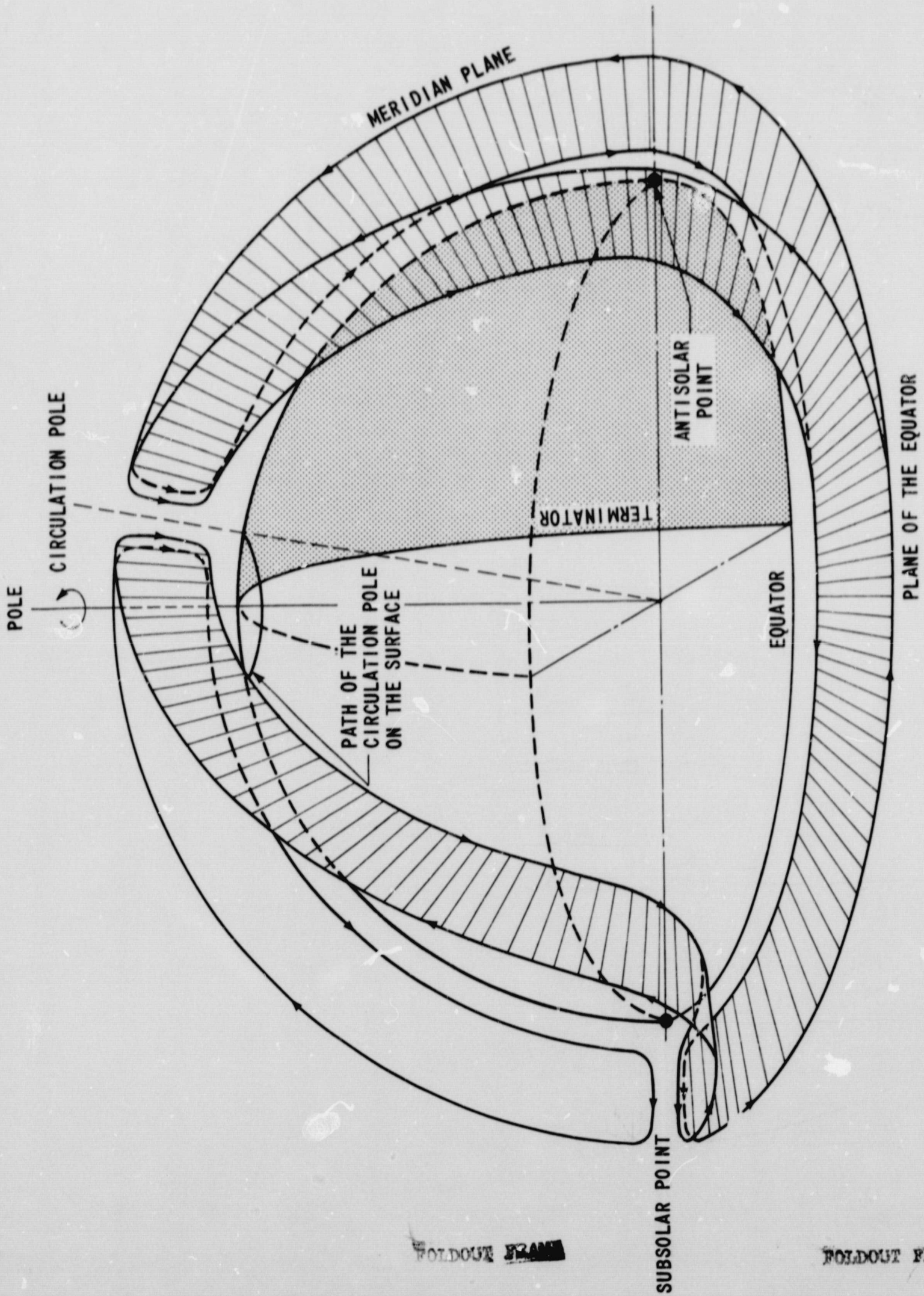


FIGURE 8 - CIRCULATION DRIVEN BY EQUATOR TO POLE AND DAY TO NIGHT TEMPERATURE GRADIENTS ALONG THE SURFACE